

## REAL CASE ISLANDING DETECTION ON THE DISTRIBUTION NETWORK BY USING MICROPMU UNITS

Miguel VERISSIMO  
EDP Distribuição - Portugal  
miguel.verissimo@edp.pt

André NEVES  
EDP Distribuição - Portugal  
andre.neves@edp.pt

João Carvalho  
EDP Distribuição - Portugal  
joao.carvalho@edp.pt

Pedro ALEIXO  
EDP Distribuição - Portugal  
pedro.aleixo@edp.pt

Miguel LOURO  
EDP Distribuição - Portugal  
miguel.louro@edp.pt

Fernando Pimenta  
Infocontrol - Portugal  
fernando.pimenta@infocontrol.pt

André FALCAO  
EDP Distribuição - Portugal  
andre.falcao@edp.pt

Celso Filipe SILVA  
EDP Distribuição - Portugal  
celsofilipe.silva@edp.pt

### ABSTRACT

*Distributed Generation (DG) is gradually increasing in Distribution Grid, both in LV, MV and HV, creating new challenges to utilities. One of them is the capacity to detect an unwanted islanding operation. As seen in recent studies, especially when the load demand is similar to generation, traditional anti-islanding detection protection functions, that rely mainly on frequency deviations and voltage variations at the interconnection point may present a low performance.*

*To suppress this constrains, new approaches are being tested, such as using the voltage phase angle difference between the main grid and the DG side. For the purpose of assessing the effectiveness of this approach EDP Distribuição (EDPD) decided to install a set of micro Phasor Measurement Units ( $\mu$ PMU) in the Interconnection point of EDP Distribuição's Energy Storage System (ESS) that is connected to a MV 15kV grid and has the capability of being able to create an 15kV network island automatically in case of an outage in the feeder or manually.*

*In this paper, voltage phase measurement is used as a parameter for islanding detection and some real islanding situations detected, using this method, are shown. Also, this paper presents some difficulties encountered during the installation and operation of  $\mu$ PMUs.*

### INTRODUCTION

The implementation of DG, usually from Renewable energy resources (RES), in the grid changed the paradigm of how the grid is operated, since distribution network power flows changed from being strictly unidirectional, to the clients, to bidirectional, with embedded generation in the grid. Additional problems have also arisen to the Distribution System Operator (DSO) regarding the grid control being one of them the occurrence of undesired islanding.

IEEE 929-2000 defined Islanding operation as "Islanding is the condition in which a portion of the utility grid that contains both load and distributed resources remain energized while isolated from the remainder of the utility

system".

Undesired islanding is a very sensitive problem to utilities because they cannot control voltage, frequency and it could lead to power quality problems, reclosing problems and damages to DG's equipment and safety hazards for the utility line workers [1]. For that reason, in IEEE 1547 standard was stipulated that an unwanted islanding operation should be detected, and the DG disconnected within 2 sec. Despite Portuguese legislation not mentioning a time interval for island clearing, EDPD has always seek to detect and disconnect any unwanted islanded system in the smallest time interval possible.

Islanding detection methods are classified into two main categories: Remote and local.

Remote techniques use SCADA system and power line communication based on gathering data from the field to convey to a central station. One of the major drawbacks of this technique is the delay, or even losses in communication, between an islanding occurrence and the detection/response of the SCADA system due to communication delays. Other issues are the high cost of the solution, that makes it inviable to disseminate widely. Local techniques can also be sub-divided into active and passive methods, depending on how they interact with the utility grid. If the method is based on signal injection on the grid it is classified as an active method. If the detection methods are based only on monitoring the grid variables, they are classified as a passive method.

One of the most common active method is the impedance detection in which a current spike is periodically injected in the interconnection point and its principal advantage is the low Non- Detection Zone (NDZ). However, the injection of signals in the grid create power quality problems and are not suitable when a significant number of DGs are connected on the same feeder.

Passive methods rely on monitoring grid variables, which make this method grid friendly and attractive to utilities from an economical point of view.

One the other hand, they are characterized by having larger NDZ when compared to the other methods, because the variation of the grid variables may be almost neglectable in situations where the mismatch between load and generation is low.

The most common techniques using Passive methods are under/over voltage and under/over frequency. The selection of these two variables are based in the premise that, in normal circumstances, if an island is formed, the

changes in voltage and frequency are going to be large. In Figure 1 is shown the Non-Detection Zone when using these two techniques.

In the latter method, the integration of micro Phasor Measurement Units ( $\mu$ PMU) could be very helpful to utilities since  $\mu$ PMUs have the capability of measuring phasor angles with a great sensitivity and quickly enough to meet the requirements imposed by IEEE 1547 [2]. In fact, PMUs can measure sequence voltages and current amplitude, phase voltages and currents, frequency and rate of change of frequency. PMUs use a GPS signal for their internal algorithm and to add a time stamp to the measured data.

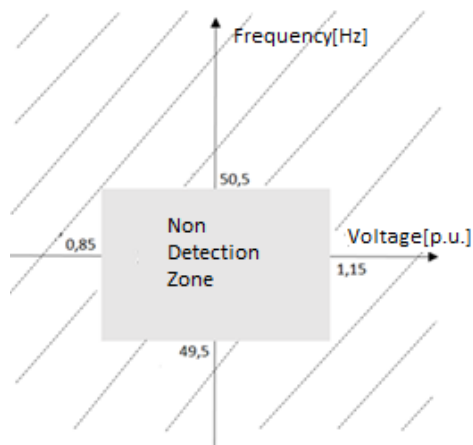


Figure 1 - The Non-Detection Zone.

## INSTALATION AND CONFIGURATION OF $\mu$ PMU

To evaluate the benefits of using  $\mu$ PMUs for islanding detection, EDP Distribuição decided to install a set of microphasors in a grid which already has the possibility of wanted islanding, creating all the necessary requirements to test the application of  $\mu$ PMUs with no impact to costumers. EDP chose the 15kV grid of Évora Substation because there is an ESS connected to this section of the grid, which can be entirely controlled by EDP and has the possibility of operating several different modes (ex.: PQ; PV), allowing for the execution of different case studies (Figure 2).



Figure 2 – EDP's ESS at Valverde, Évora.

One  $\mu$ PMU was installed on the grid side,  $\mu$ PMU1, and the other one on the DG side,  $\mu$ PMU2. The representation of the actual configuration is present on Figure 3.

Due to space limitation, and because both  $\mu$ PMUs are geographically on the same site, only one GPS receiver was installed. A cable splitter was used for that purpose. Nevertheless, the use of only one GPS receiver implied a lower signal quality, which could result on imprecise estimates of the phase variables. Regarding Phasor Data Concentrator (PDC) connection, IEEE C37.118 protocol was used via 4G.

EDPD decided to measure only phase and magnitude of voltages. Current measurements were left out due to the need for extra hardware and because the use cases did not comprise current measurements.

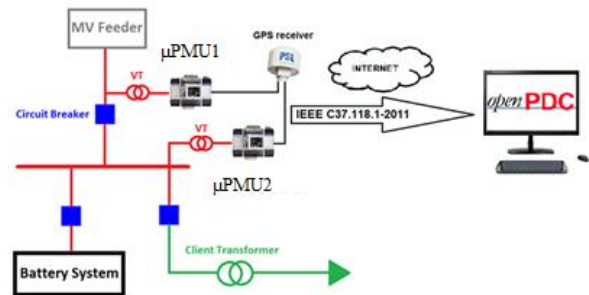


Figure 3 – Connection Diagram of EDP's PMU.

In Table 1 the settings applied to the  $\mu$ PMU are presented, including the voltage ratio in the primary and secondary windings of the potential transformer and the rated frequency of the Electrical grid.

Table 1 – Configuration Settings of  $\mu$ PMU.

$\mu$ PMU Configuration	
Rated frequency [Hz]	50
Potential transf. Ratio	8660.254:57.735
Phasor measurements/sec	10
C37 reporting rate [frames/sec]	10

For the selection of the streaming of phasor measurements per second, it is possible to choose between 10, 25, 50 and 100. A more precise estimate of the phase variables is obtained with a greater number of measurements/sec. However, that highly increases the need for storage and  $\mu$ PMU have limited internal memory. In addition, it was found in the preliminary tests that the gain is not relevant. Considering C37 reporting rate, a value of 10 frames per second was chosen in accordance to the number of measurements/second that were also defined to be 10. An important issue that needs to be considered when choosing the number of frames/second, is the wireless telecommunication signal strength. In this case, ESS is located at a site where the 4G signal strength is low,

restraining the data streaming speed and therefore choosing the lowest communication rate is the best option. Furthermore, a higher rate sampling rate would not bring benefits for the use cases being tested.

### REAL-CASE ISLANDING EVENTS

An open source application for processing streaming time-series data in real-time, OpenPDC, was used. This application is constantly receiving data, from the  $\mu$ PMU, to detect an islanding formation based on the measurements obtained by the synchrophasors.

OpenPDC offers the possibility of not only processing data but also creating new signals based on measurements and generating alarm signals using measurements comparisons or thresholds.

### Method used for islanding detection

For detecting an islanded system, a method based on the phase angle difference between  $\mu$ PMU1 and  $\mu$ PMU2 was implemented. The angle measured by the  $\mu$ PMU1 was chosen as the angle reference. If the phase angle difference is greater than a defined value, then an alarm signal is generated. The algorithm for the islanding detection is represented in Figure 4.  $\Theta_{th}$  represents the threshold angle, phase angle limit difference, and it was set to be 20 degrees. In some previous studies, the angle difference is defined to be between 30° and 60° [3]. However, in this case, since the  $\mu$ PMU are installed in the same bus and the ultimate purpose is to generate an alarm, it was decided to set a lower angle.

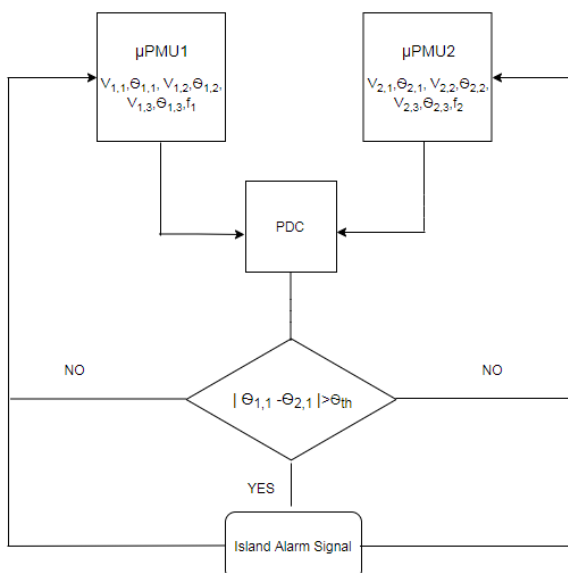


Figure 4 - Islanding detection algorithm.

### First Case: 23<sup>rd</sup> of September 2018

On the 23<sup>rd</sup> of September there was an island formation

due to an outage on the 15kV grid of Évora. That event was detected by the islanding detection algorithm. The incident was a Phase-to-Ground fault, on the MV line that connects Évora Substation to the Energy Storage System. During the power outage from the grid side, ESS was able to supply the load, originating an islanded system with an approximate duration of 50 seconds, before being reconnect to the grid. The main outage events are shown in Table 2. In Figure 5 is shown the behavior of the phase voltages during the event.

Table 2 - Events of incident of the 23rd of September

ID	Time	Description
1	03:07:52	15kV line outage; Line circuit breaker trips
2	03:07:53	ESS discharging and Mode VF active
3	03:08:08	Line voltage returned; circuit breaker remained open
4	03:08:56	Line circuit breaker was closed; End of island

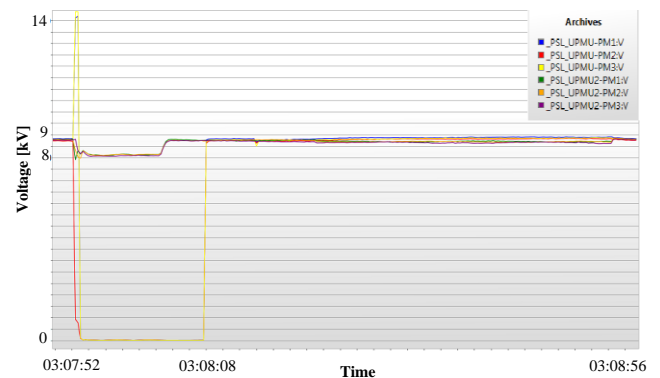


Figure 5 - Behavior of the phase voltages during the 1st outage.

The phase angle difference and its corresponding alarm are present in Figure 6, where the phase angle difference is represented by the blue line and the alarm signal by the red one.

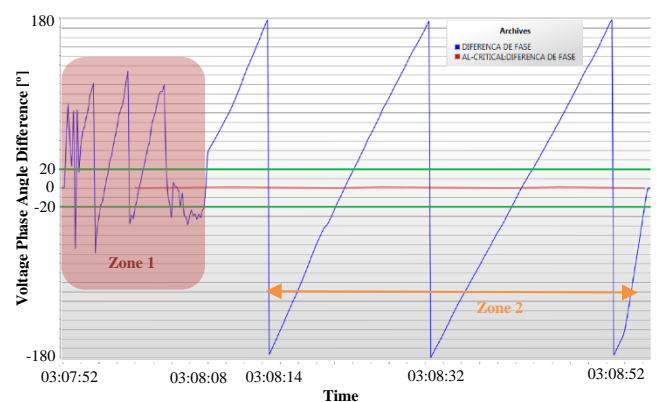


Figure 6 - Phase Angle Difference and Alarm Signal during the outage.

By Figure 6 it is possible to detect two distinct zones: one, occurring during events ID 2 to 3, in which phase angle

difference signal behaves in an abnormal way, since  $\mu$ PMU1 has no voltage measurements; a second zone, where the ESS is in islanding operation but there is a voltage on the MV feeder side. In this case the phase angle difference between to isolated systems showed a triangular waveform.

From Figure 6 it is also possible to notice that the alarm signal (red line) starts around 3:08:00, and not right after event ID 2, because a delay time was set.

Regarding frequency, as it can be seen in Figure 7, the frequency measured by the  $\mu$ PMU1 is strictly greater than the one obtained by  $\mu$ PMU2.

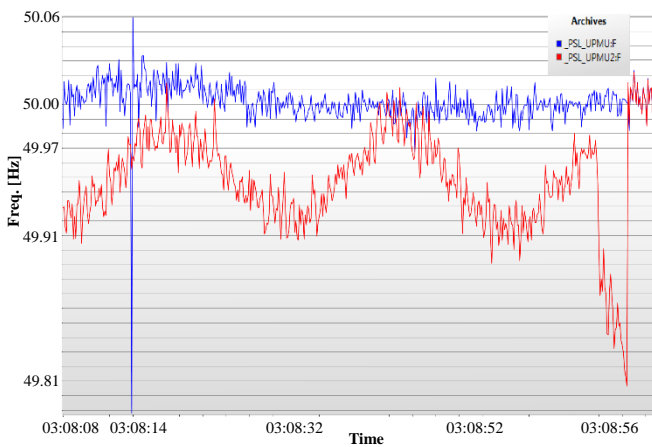


**Figure 7** - Frequency of  $\mu$ PMU1 and  $\mu$ PMU2 during the 1st outage.

It can be noted on Figure 6 that the slope of the phase angle difference is positive since the frequency of  $\mu$ PMU1, considered as reference, is greater than the one measured by  $\mu$ PMU2, hence making the phase voltage of  $\mu$ PMU2 lagging the one of  $\mu$ PMU1.

### **Second Case: 16th of October 2018**

Like the first case, in the 16<sup>th</sup> of October an island was automatically formed due to a fault in the upstream grid causing a voltage dip that caused the ESS to automatically form an island. The description of the events of the incident are presented in Table 3.

**Table 3** - Events description of incident of 16th of October.

ID	Time	Description
1	23:59:14	Voltage dip; Circuit breaker trips
2	23:59:15	ESS discharging and Mode VF active
3	23:59:15	Line voltage returned; circuit breaker remained open
4	23:59:22	Storage circuit breaker trip; End of island
5	00:00:15	Line Circuit breaker closed

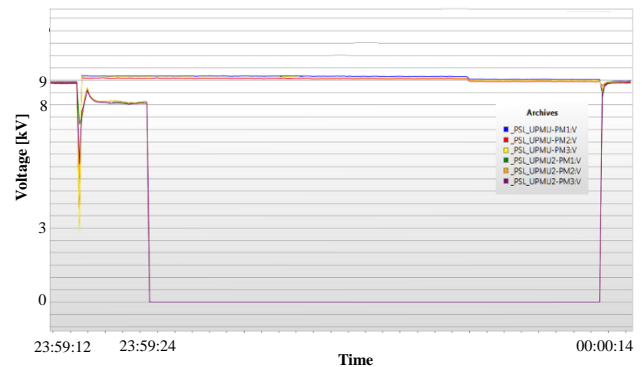


**Figure 8** - Behavior of the phase voltages during the 2<sup>nd</sup> outage.

Since the duration of this island was much shorter than in first case, as it can be seen in Table 3 and in Figure 8, the alarm signal only started to be active by the end of the island duration. This is in part explained by the decision to use a delay of 3 seconds between the phase angle difference and the generation of the alarm signal. In Figure 9 is shown the evolution of the phase angle difference, blue line, and the alarm signal, red line.

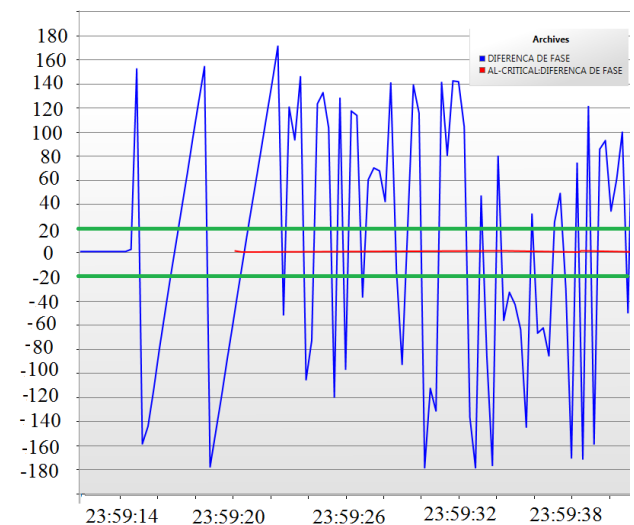


**Figure 9** - Evolution of phase angle difference and alarm signal during the 2<sup>nd</sup> outage.

During this islanding operation, the form of the phase angle difference is alike to the second zone referred on Figure 6, however the triangle form is not so well defined., because of short-time island operation. After ID event 4 occurs, it is possible to notice a change on the behavior of the phase angle difference, starting to change in an abruptly manner due to the absence of voltage on  $\mu$ PMU. The frequency measured on  $\mu$ PMU1 and  $\mu$ PMU2 are presented on Figure 10. It can be seen, that both frequencies are inside the limits of the NDZ zone, represented on Figure 1, considering the tradition anti-islanding detection methods. Also, as mentioned for the previous case, the frequency measured by  $\mu$ PMU1, in blue, is greater than of  $\mu$ PMU2, in red, and therefore the positive



slope of the phase angle difference.

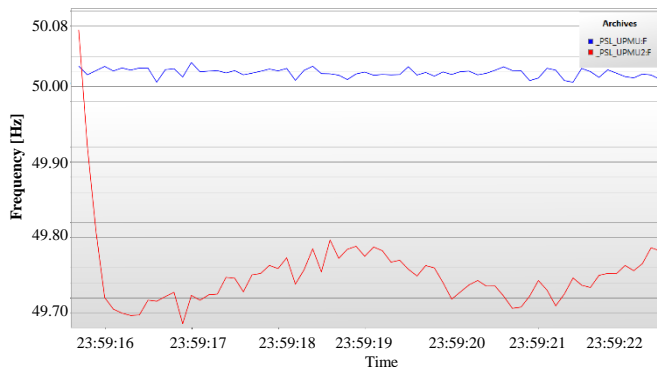


**Figure 10** - Frequency measured on  $\mu$ PMU1 and  $\mu$ PMU2. during the 2<sup>nd</sup> outage.

## CHALLENGES FOUND IN THE USAGE OF $\mu$ PMU IN GRID OPERATION

In this pilot experience with the testing of  $\mu$ PMUs in the grid there were lessons learned, not only regarding the installation of the  $\mu$ PMUs but also with the deployment of a new anti-island detection method.

One of the major challenges was the difficulty to establish a stable communication between  $\mu$ PMUs and the PDC, due in part to the utilization of a virtual private network over a wireless communication channel, which resulted in a slower data rate, but mostly because the ESS site was located on a local with a low 4G signal strength. Due to space and technical limitation, the team was forced to install only one GPS receiver on ESS for both  $\mu$ PMUs, which had a negative impact on the quality of the measurements due to the level of precision of the time stamp. When there are uncertainties on the timestamp,  $\mu$ PMUs issues a quality signal, QF. In Table 4 and Table 5 are shown the rate of failure of the signal for 11 days.

**Table 4** - Rate of failure of  $\mu$ PMU1.

Date	QF=1	QF=0	Rate of failure [%]
14-10-2018	759694	759694	50
16-10-2018	156513	623312	20,07
17-10-2018	55647	789349	6,59
20-10-2018	41633	812000	4,88
22-10-2018	46432	803533	5,46
31-10-2018	83149	792023	9,50
25-10-2018	42752	801069	5,07
27-10-2018	40290	818985	4,69
29-10-2018	56789	779771	6,79
30-10-2018	50399	805104	5,89
01-11-2018	43462	810995	5,09

**Table 5** - Rate of failure of  $\mu$ PMU2.

Date	QF=1	QF=0	Rate of failure [%]
14-10-2018	701064	701064	50,00
16-10-2018	164303	672246	19,64
17-10-2018	40537	803048	4,81
20-10-2018	54663	803414	6,37
22-10-2018	41010	810615	4,82
31-10-2018	49810	792023	5,92
25-10-2018	49389	801069	5,81
27-10-2018	38650	818985	4,51
29-10-2018	68380	779771	8,06
30-10-2018	38470	805104	4,56
01-11-2018	32305	810995	3,83

## CONCLUSIONS

With this experience, EDPD concluded that the integration of  $\mu$ PMUs in the grid is an effective way for detecting islanding, due to the easiness of implementation and a greater detection probability than other methods. This facilitates the detection of islanding operations within the time limit defined by international standards.

Phase difference detection mechanism should be improved using smoothing filtering and an algorithm (like CUSUM, for example) that could provide a faster detection with a low probability of false alarms.

However, there is still some limitations that need to be overcome like low wireless signal strength issues, and site implementation limitations like the ones experienced in Évora pilot site. Also, there is the need of creation a communication between the PDC and automatic circuit breaker action to insure a proper disconnection of the DG in case of an islanding operation.

## REFERENCES

- [1] A. Timbus, A. Oudalov and C.N.M.Ho, 2010, "Islanding detection in smart grids", *Proc. 2010 IEEE Energy Conversion Congress and Exposition (ECCE)*, pp. 3631-3637
- [2] "1547-2003 – IEEE Standard for Interconnecting Distributed Resources With Electric Power Systems," 2003
- [3] A. Timbus, A. Oudalov and C.N.M.Ho, 2010, "Anti-Islanding today, Successful Islanding in the Future", *Proc. 2010 IEEE Energy Conversion Congress and Exposition (ECCE)*, pp. 3631-3637
- [4] D. Lavery, D. J. Morrow, R. Best and M. Cregan, 2011, "Anti-Islanding Detection using Synchrophasors and Internet Protocol Telecommunications", *Proc. 2011 2nd IEEE PES International Conference and Exhibition on*, vol., pp.1-5